CONVOLUTIONAL BEAMSPACE USING IIR FILTERS

Po-Chih Chen and P. P. Vaidyanathan

Dept. of Electrical Engineering, MC 136-93
California Institute of Technology, Pasadena, CA 91125, USA
pochih@caltech.edu, ppvnath@systems.caltech.edu

ABSTRACT

The recently introduced convolutional beamspace (CBS) method has some advantages over traditional beamspace methods in array processing. This paper introduces a variant which uses IIR instead of FIR filters in the convolutional layer. In CBS, the sources falling in the stopband are assumed to be sufficiently attenuated so that we can identify the passband DOAs. An IIR filter often requires a much lower order for the same set of magnitude response specifications. Hence, the computational complexity of IIR-CBS can be smaller than FIR-CBS. Moreover, IIR-CBS can even give smaller DOA estimation errors than FIR-CBS because the longer FIR filter length means shorter steady-state filter output length, which leads to larger estimation errors. The advantages of IIR-CBS are verified by numerical examples.

Index Terms— Convolutional beamspace, IIR filters, root-MUSIC, ESPRIT

1. INTRODUCTION

While beamspace processing [1–10] has been well-known to array signal processing researchers, convolutional beamspace (CBS) for direction of arrival (DOA) estimation is fairly recent [11–14]. CBS has all the benefits of classical beamspace methods: (a) lower computational complexity, (b) higher resolution of closely spaced DOAs [4–6], and (c) smaller bias [7, 12]. And it offers more: in classical beamspace, the Vandermonde structure of the output of a uniform linear array (ULA) is lost, which mandates additional preprocessing before applying subspace methods like (root-)MUSIC [7] or ESPRIT [8]. But CBS preserves the Vandermonde structure, allowing subspace methods to be directly applied.

In a nutshell, CBS uses a spatial finite-impulse-response (FIR) filter $H(z)$ to restrict the ULA output to an angular sector. The "CBS trick" is to retain only the *steady-state* part of the output, whereby the Vandermonde structure is preserved. Uniform decimation is then used for dimensionality and complexity reduction, after which we can readily estimate DOAs using subspace methods.

A natural question is whether we can use infinite-impulse-response (IIR) filters instead of FIR. We explore this in this paper. While the idea of using IIR filters instead of FIR might seem minor, there are some nontrivial details as we shall see. Also, IIR filtering has not been widely used in array processing in the past. With large arrays becoming more prevalent today [15, 16], perhaps the time has come for more widespread use of IIR methods. They are certainly very promising for CBS-based DOA estimation as we shall see.

This work was supported by the Office of Naval Research grant N00014-21-1-2521, and the California Institute of Technology.

In CBS, even for large arrays the FIR filter length L has to be small compared to the number of sensors N. The reason is that the MSE of DOA estimates is approximately proportional to $(N-L+1)^{-3}$ as shown in [12]. (This is because the effective output length is $N-L+1$ after discarding the transient samples.) So FIR-CBS has larger estimation errors as L gets closer to N. On the other hand, with small L we cannot produce very sharp transition bands. This is where IIR filters help. They not only produce beamspace filters with sharper transition bands, they are also more economic than FIR filters (i.e., a much smaller filter order is required). That is, IIR-CBS has lower computational complexity. Furthermore, IIR-CBS can achieve smaller DOA estimation errors than FIR-CBS. This is because the region where the transient component of IIR filters is significant is typically smaller than the transient duration in the FIR case as we shall see. These advantages of IIR-CBS will be verified by numerical examples.

Paper outline: The CBS method is reviewed in Sec. 2, and IIR-CBS is introduced in Sec. 3. Sec. 4 demonstrates the advantage of IIR-CBS using simulations. Sec. 5 concludes the paper.

2. PRELIMINARIES

The signal model is as in [12]: an N-sensor uniform linear array (ULA) receives D plane waves, all with a single wavelength λ. The interelement spacing is $\lambda/2$ and the signal produced by the array is

$$\mathbf{x} = \mathbf{A}\mathbf{c} + \mathbf{e}, \tag{1}$$

where $\mathbf{A} \in \mathbb{C}^{N\times D}$, with kth column $\mathbf{a}_N(\omega_k) = [1\ \alpha_k\ \cdots\ \alpha_k^{N-1}]^T$, $\alpha_k = e^{j\omega_k}$. Here $\omega_k = \pi \sin\theta_k$, where θ_k are the DOAs measured from a line normal to the ULA. The ULA ensures that $\mathbf{a}(\omega)$ and $\mathbf{A}$ have Vandermonde structure. The source amplitudes in $\mathbf{c}$, and noise $\mathbf{e}$ satisfy $E[\mathbf{c}] = \mathbf{0}$, $E[\mathbf{e}] = \mathbf{0}$, $E[|c_i|^2] = p_i$, $E[\mathbf{e}\mathbf{e}^H] = \sigma_e^2\mathbf{I}$, and $E[\mathbf{c}\mathbf{e}^H] = \mathbf{0}$.

In traditional convolutional beamspace (CBS) [12], the ULA output $x(n), 0 \le n \le N-1$ is filtered with an FIR filter $H(z) = \sum_{n=0}^{L-1} h(n)z^{-n}$ to obtain the output $y(n)$. That is, the z-transform of $y(n)$ can be computed as [17]

$$Y(z) = H(z)X(z) \tag{2}$$

where $X(z) = \sum_{n=0}^{N-1} x(n)z^{-n}$. Here $L < N$ and we retain only the *steady-state* part $\mathbf{y} = [y(L-1)\ y(L)\cdots y(N-1)]^T$, so that $\mathbf{y}$ can also be written as in (1) with an adjusted matrix $\mathbf{A}_L$ in place of $\mathbf{A}$. This $\mathbf{A}_L$ *still enjoys the Vandermonde property*—this is a crucial difference from standard

beamspace [7]—and allows CBS to use (root-)MUSIC and ESPRIT directly on $\mathbf{y}$. As shown in [12], $\mathbf{y}$ is given by

$$\mathbf{y} = \mathbf{A}_L\mathbf{d} + \mathbf{H}\mathbf{e}, \tag{3}$$

where $\mathbf{A}_L$ is the submatrix of $\mathbf{A}$ containing the first $N - L + 1$ rows of $\mathbf{A}$, and $\mathbf{H}$ is the convolution matrix as in [12]. The elements of $\mathbf{d}$ satisfy $|d_k| = |H(e^{j\omega_k})c_k|$. Thus the kth source amplitude c_k is weighted by the frequency response $H(e^{j\omega})$ at $\omega = \omega_k$. For a good filter $H(e^{j\omega})$, $\mathbf{y}$ *represents only sources* ω_k *in the passband of* $H(e^{j\omega})$. For large arrays, the filter length $L < N$ can be reasonably large, and out-of-band sources can be suppressed effectively.

The well-known complexity advantage of beamspace is achieved in CBS by decimating $y(n)$ by M, where the passband of $H(e^{j\omega})$ is $|\omega| < \pi/M$ (or a shifted version of this). This reduces the size of $\mathbf{y}$ approximately by a factor of M, reducing the complexity of eigenspace computation from $O(N^3)$ to $O(J^3)$ where $J = \lfloor (N - L + 1)/M \rfloor$. In practice, we wish to avoid wastage of hard earned data, while at the same time reducing complexity. For this, we simply create M separate decimated versions of $y(n)$ by successively shifting before decimation. The details can be found in [12]. For each decimated version, we have an output equation of the form

$$\mathbf{v}_l = \mathbf{A}_{\rm dec}\mathbf{d}_l + \mathbf{D}_l\mathbf{H}\mathbf{e}, \quad l = 0, \ldots, M-1, \tag{4}$$

where $\mathbf{A}_{\rm dec}$ is the "decimated" array manifold matrix of smaller size $J \times D$ and the elements of $\mathbf{d}_l$ satisfy $|d_{l,k}| = |H(e^{j\omega_k})c_k|$. Here $\mathbf{D}_l$ is an appropriate decimation matrix [12]. The kth column of $\mathbf{A}_{\rm dec}$ is the $J \times 1$ Vandermonde vector $[1 \;\; e^{jM\omega_k} \;\; e^{j2M\omega_k} \cdots]^T$. The fact that only the DOAs in the passband of $H(e^{j\omega})$ affect the data $y(n)$ can be used to remove ambiguities caused by the presence of $e^{jM\omega}$ (instead of $e^{j\omega}$) in $\mathbf{A}_{\rm dec}$ [12]. By estimating the $J \times J$ covariance of $\mathbf{v}_l$ and averaging over l, we make sure no data has been wasted. We use a finite number of snapshots of array outputs to estimate the covariance in practice.

In addition to reducing complexity from $O(N^3)$ to $O(J^3)$ like traditional beamspace, CBS also allows more effective attenuation of out-of-band sources for large arrays. This often leads to better estimation of DOAs for correlated sources [12]. We will see that by using IIR filters instead of FIR, we can add to the advantages to CBS. Namely, we reduce filtering complexity further, and improve estimation accuracy.

3. CBS USING IIR FILTERS

In this paper, we propose to use an IIR filter

$$H(z) = \frac{P(z)}{D(z)} = \sum_{n=0}^{\infty} h(n)z^{-n} \tag{5}$$

in (2), where $P(z)$ and $D(z)$ are degree-R polynomials in z^{-1}. The motivation is that an IIR filter often requires a much lower order for the same set of magnitude response specifications [18]. This can lead to lower computational complexity and better DOA estimation performance, as we shall see later. The filter $H(z)$ can be designed as any standard IIR filter such as a (discrete-time) Chebyshev filter or elliptic filter [17, 18]. In the traditional FIR-CBS, there are only a finite number $L - 1$ of transient output samples $y(0), \ldots, y(L - 2)$ before reaching steady state, so we simply discard these samples in order to preserve the Vandermonde structure of the ULA. Now in IIR-CBS, since the filter is infinitely long, strictly speaking, there is no steady state. However, typically $|h(n)|$ decays as n increases. Suppose it decays to a negligible level after $n \geq L_{\rm I}$. Then we can similarly discard the $L_{\rm I} - 1$ output samples $y(0), \ldots, y(L_{\rm I} - 2)$ and define $\mathbf{y} = [y(L_{\rm I} - 1) \;\; y(L_{\rm I}) \cdots y(N-1)]^T$ as the IIR-CBS output signal. Then the Vandermonde structure is approximately preserved because for $L_{\rm I} - 1 \leq n \leq N - 1$, we have

$$y(n) = \sum_{i=1}^{D} c_i H(e^{j\omega_i})e^{j\omega_i n} + q(n) + \sum_{k=0}^{n} h(k)e(n-k), \tag{6}$$

where $q(n) = \sum_{k=n+1}^{\infty} h(k) \sum_{i=1}^{D} c_i e^{j\omega_i(n-k)}$ is negligible. Thus, ignoring the noise term, we have

$$\mathbf{y} \approx \mathbf{A}_{L_{\rm I}}\mathbf{d}', \tag{7}$$

where $\mathbf{d}'$ has elements $d'_k = c_k e^{j(L_{\rm I}-1)\omega_k} H(e^{j\omega_k})$. This is similar to (3). Hence, we can decimate $\mathbf{y}$ and estimate DOAs based on the average covariance $\mathbf{R}_{\rm ave}$ of the decimated outputs using standard methods like root-MUSIC.

Now we compare the computational complexity of IIR-CBS and FIR-CBS. Suppose root-MUSIC is used to estimate DOAs. Then we need to do filtering, eigenvalue decomposition of $\mathbf{R}_{\rm ave}$, and root-finding. Given K snapshots of the N-sensor ULA output, Table 1 shows the total complexity for IIR-CBS with filter order R and for FIR-CBS with filter length L. In the expressions in Table 1, the first term (KNR or KNL) is the filtering complexity, and the second term is the eigendecomposition complexity. The complexity for root-finding is $O(n^2 \log n)$ [19], where $n = (N - L_{\rm I} + 1)/M$ for IIR-CBS and $n = (N - L + 1)/M$ for FIR-CBS, so it is ignored in the big-O notation. As mentioned earlier, an IIR filter often requires a much lower order, i.e.,

$$R \ll L, \tag{8}$$

for the same set of magnitude response specifications [18]. Hence, the complexity of IIR-CBS is typically much smaller than that of FIR-CBS, especially for large arrays (large N), which are becoming increasingly important [15, 16]. In Table 1, we also show numerical values by setting the parameters as in Examples 1 and 2 in Sec. 4. In both examples, $K = 500$, $N = 99$, $R = 5$, and $M = 4$. In Example 1, $L_{\rm I} = 12$ and $L = 20$. In Example 2, $L_{\rm I} = 16$ and $L = 56$. The numbers are computed exactly from the expressions in Table 1 without considering the hidden constant factors in the big-O notation. IIR-CBS indeed has much smaller complexity. In Sec. 4, we show that with less complexity, IIR-CBS can achieve similar or even better DOA estimation performance than FIR-CBS.

Table 1: Complexity of IIR-CBS and FIR-CBS

	Complexity	Example 1	Example 2
IIR-CBS	$O\Big(KNR + \big(\frac{N-L_{\rm I}+1}{M}\big)^3\Big)$	258,148	256,761
FIR-CBS	$O\Big(KNL + \big(\frac{N-L+1}{M}\big)^3\Big)$	998,000	2,773,331

IIR-CBS is particularly advantageous over FIR-CBS when we want to design a filter with a narrow transition band. This reduces the probability of a DOA appearing in the transition band, so it is of practical interest. An FIR filter requires

a very large filter length L to have good stopband attenuation in this case, which means the effective filter output length $N-L+1$ will be small. Since the MSE of DOA estimates is approximately proportional to $(N-L+1)^{-3}$ as shown in [12], FIR-CBS will suffer large estimation error. By contrast, an IIR filter requires a relatively small order R, and we can also choose a reasonably small $L_{\rm I}$ to get good estimation performance. Such advantage will be verified by a numerical example in Sec. 4. The nonlinear phase response of IIR filters does not have a significant effect on the MSE of DOA estimates because the MSE mainly depends on the power of the source but not phase of the source amplitude [12].

Remarks: 1) The IIR filter $H(z)=P(z)/D(z)$ can be implemented with R multipliers, as explained below. A wide family of IIR filters, including Butterworth, Chebyshev, and elliptic filters, can be represented as

$$H(z)=[A_0(z)+A_1(z)]/2, \tag{9}$$

where $A_0(z)$ and $A_1(z)$ are stable unit-magnitude allpass filters [18,20,21], and their orders r_0 and r_1 satisfy $r_0+r_1=R$. Moreover, if the filter order R of $H(z)$ is odd, then $A_0(z)$ and $A_1(z)$ have real coefficients. Since a real coefficient allpass filter with order r can be implemented with r multipliers [18], we can implement (9) with R multipliers. We always use an odd R in this paper.

2) In [12], it was shown that the noise term after filtering and decimation can be whitened if $H(z)$ is a spectral factor of a Nyquist(M) filter $G(z)$ (i.e., the impulse response of $G(z)$ satisfies $g(Mn)=\delta(n)$ where $G(z)$ is such that $G(e^{j\omega})=|H(e^{j\omega})|^2$). This makes it easy to find the noise eigenspace by computing eigenvectors of $\mathbf{R}_{\rm ave}$, which is what we do in simulations. We can also design an IIR filter $H(z)$ to be a spectral factor of an IIR Nyquist(M) filter to whiten the noise. There are many ways to design such filters [22–25]. But in many cases, if $H(z)$ is a "good" IIR filter with total passband width $\approx 2\pi/M$ and ripples properly constrained, this Nyquist property is approximately satisfied, that is,

$$\max_{n\neq 0}|g(Mn)| \ll g(0) \quad \text{(nearly-Nyquist property)}. \tag{10}$$

For simplicity, this is what we use in simulations.

4. SIMULATIONS

Example 1: We compare IIR-CBS for DOA estimation with FIR-CBS and element-space (i.e., directly using $\mathbf{x}$ to estimate DOAs). Consider a ULA with $N=99$ sensors. There are 3 in-band (passband) sources with DOAs $\theta=-5^\circ,0^\circ,5^\circ$, and 3 out-of-band (stopband) sources with DOAs $\theta=40^\circ,60^\circ,80^\circ$. Each in-band source has power 0 dB, each out-of-band source has power 20 dB, and the noise variance is $\sigma_e^2=5$ dB. Sources n and $n+3$ have a correlation coefficient $\rho=0.9$ for $n=1,2,3$. The decimation ratio is $M=4$. For IIR-CBS, $H(z)$ is designed to be a lowpass Chebyshev (type 2) filter with order $R=5$. For this filter, $\max_{n\neq 0}|g(Mn)|\approx 0.001g(0)$, so it indeed satisfies the nearly-Nyquist property (10). For FIR-CBS, $H(z)$ is designed to be a spectral factor of a lowpass Nyquist-equiripple filter [26]. The transition band for each filter is $\omega\in[0.125\pi,0.375\pi]$. The parameter $L_{\rm I}$ for IIR-CBS and the FIR filter length L are varied in this experiment. Magnitude responses of the IIR filter and FIR filters with some typical lengths L used are shown in Fig. 1(a). The stopband attenuation of the IIR filter with order 5 is as good as that of the FIR filter with length 20. The stopband attenuation of the FIR filter with a shorter length, e.g. 8, is not so good. Then we perform DOA estimation using root-MUSIC. The number of DOAs is assumed known. Covariance estimates are obtained by using 500 snapshots, and we average 500 Monte Carlo runs to get the plot. Fig. 1(b) shows root mean square error (RMSE) obtained by averaging square errors measured in ω over all in-band DOAs, as we vary L or $L_{\rm I}$. For IIR-CBS, there is an optimal $L_{\rm I}$, 12 in this case, that gives the smallest RMSE. When $L_{\rm I}$ is too small, RMSE increases because the first few samples suffer from a significant transient effect due to the typically large $|h(n)|$ for small n. When $L_{\rm I}$ is too large, RMSE increases because we discard too many filter output samples and the effective output length $N-L_{\rm I}+1$ is too small. For FIR-CBS, there is also an optimal L, 20 in this case, that gives the smallest RMSE. When L is too small, RMSE increases because the filter stopband attenuation is not good enough to suppress the out-of-band sources. When L is too large, RMSE increases because the effective filter output length is small. In this example, the RMSE of IIR-CBS is a lower bound for the RMSE of FIR-CBS. Moreover, for each simulation point when $L_{\rm I}=L\geq 12$, the computational complexity of IIR-CBS is smaller than that of FIR-CBS. That is, IIR-CBS is better in terms of both complexity and estimation performance. Meanwhile, when $L_{\rm I}$ and L are properly chosen, the RMSEs of both IIR-CBS and FIR-CBS are smaller than element-space and close to the element-space Cramer-

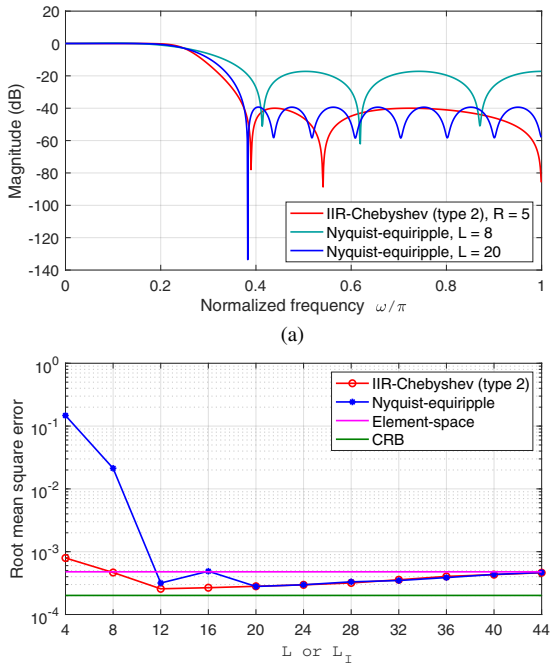

Fig. 1: Performance of IIR-CBS using Chebyshev (type 2) filter for various $L_{\rm I}$, FIR-CBS using Nyquist-equiripple filter for various L, and element-space. The IIR filter order is fixed at $R=5$. (a) Responses of IIR and FIR filters used. The transition band for each filter is $\omega\in[0.125\pi,0.375\pi]$. (b) RMSE of DOA estimates as we vary L for FIR-CBS (or $L_{\rm I}$ for IIR-CBS). Element-space CRB is also plotted.

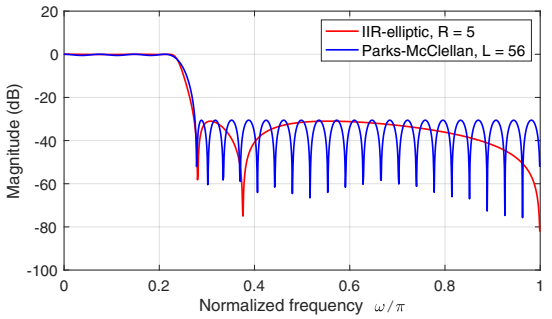

(a)

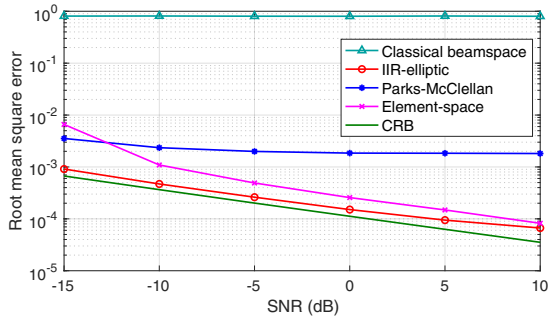

(b)

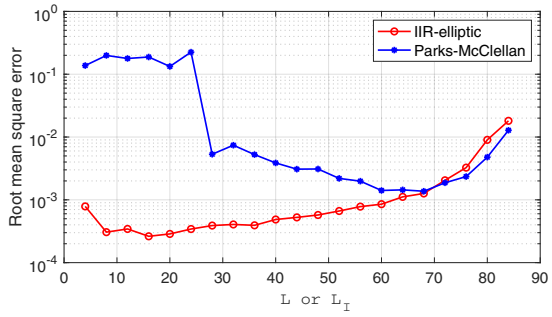

(c)

Fig. 2: Performance of IIR-CBS using elliptic filter, FIR-CBS using Parks-McClellan filter, classical beamspace, and element-space. The IIR filter order is fixed at $R = 5$. (a) Responses of IIR and FIR filters used. A narrow transition band $\omega \in [0.225\pi, 0.275\pi]$ is used for each filter. (b) RMSE of DOA estimates as we vary SNR. The IIR and FIR filters in (a) are used. We set $L_{\rm I} = 16$ for the IIR filter. Element-space CRB is also plotted. (c) RMSE of DOA estimates as we vary L for FIR-CBS (or $L_{\rm I}$ for IIR-CBS).

Rao bound (CRB) [27] (i.e., CRB based on the original array output $\mathbf{x}$). Element-space typically has larger errors for correlated sources [12]. Even though element-space CRB cannot be larger than beamspace CRB, it is possible for element-space MSE to be larger than beamspace MSE, see [12].

Example 2: We consider an example where CBS filters have a narrow transition band, $\omega \in [0.225\pi, 0.275\pi]$. All simulation parameters are the same as in the first example unless mentioned otherwise. For IIR-CBS, $H(z)$ is designed to be a lowpass elliptic filter with order $R = 5$. For this filter, $\max_{n\neq 0} |g(Mn)| \approx 0.04 g(0)$, so it satisfies (10). For FIR-CBS, $H(z)$ is designed to be a Parks-McClellan filter [17]. Magnitude responses of the IIR and FIR filters used are shown in Fig. 2(a). The stopband attenuation of the IIR filter with order 5 is as good as that of the FIR filter with length 56. IIR-CBS can thus obtain significant complexity reduction. Then we perform DOA estimation using root-MUSIC. Fig. 2(b) shows RMSE of in-band DOA estimates for CBS using the IIR and FIR filters in Fig. 2(a) and element-space, as we vary SNR ($= 1/\sigma_e^2$). We set $L_{\rm I} = 16$ for the IIR filter. Here we also show the RMSE of classical beamspace using a 99×25 DFT matrix beamformer [7]. (Note that $25 \approx 99/M$.) The poor performance of classical beamspace is due to numerical sensitivity issues for a moderately large N as mentioned in [7]. RMSE of FIR-CBS is relatively large because the large $L = 56$ means the effective filter output length $N - L + 1$ is small. However, the RMSE of IIR-CBS is the smallest and close to the element-space CRB. The gap between the IIR-CBS RMSE and CRB gets a bit larger as SNR increases because the fixed error term $q(n)$ in (6) does not depend on the noise. This example shows the benefit of introducing IIR filters in CBS because FIR-CBS does not work better than element-space, but IIR-CBS does. In fact, FIR-CBS has larger RMSE than IIR-CBS for a wide range of L. We vary L or $L_{\rm I}$ in Fig. 2(c) while fixing $\sigma_e^2 = 5$ dB. Since we want a narrow transition band in this example, a much larger length L is required for the FIR filter to have enough stopband attenuation to suppress the out-of-band sources, but a large L results in a small effective filter output length and large RMSE. By contrast, an IIR filter needs only a small order to have enough stopband attenuation, so it is possible to get much smaller RMSE.

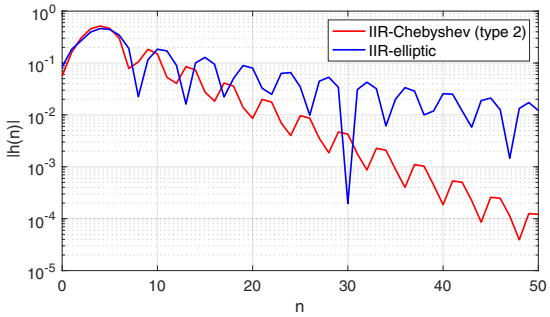

Fig. 3: Magnitude of impulse responses of the Chebyshev filter in Fig. 1(a) and elliptic filter in Fig. 2(a).

Finally, Fig. 3 shows the impulse responses of the Chebyshev filter in Fig. 1(a) and elliptic filter in Fig. 2(a). The impulse response of the Chebyshev filter decays faster than that of the elliptic filter. This explains why the optimal $L_{\rm I} = 12$ in Fig. 1(b) is smaller than the optimal $L_{\rm I} = 16$ in Fig. 2(c). We can discard less output samples for the Chebyshev filter.

5. CONCLUSION

A new variant of CBS using IIR filters is introduced. Since an IIR filter typically requires a much lower order for the same set of magnitude response specifications, smaller complexity and better estimation performance can be obtained compared to FIR-CBS, as verified in simulations. A remark is that for FIR-CBS, we can consider nonlinear phase filters instead of linear phase filters like Parks-McClellan in order to decrease the filter order for comparable magnitude response. The last numerical example shows how an optimal $L_{\rm I}$, which controls the number of discarded filter output samples, is related to the filter impulse response. A topic for future investigation would be to find a more systematic way to choose $L_{\rm I}$.

6. REFERENCES

[1] G. Bienvenu and L. Kopp, "Decreasing high resolution method sensitivity by conventional beamformer preprocessing," in *Proc. IEEE Intl. Conf. Acoust., Speech, and Signal Process.*, Mar. 1984, pp. 714–717.

[2] K. M. Buckley and X. L. Xu, "Reduced-dimension beam-space broad-band source localization: preprocessor design," in *Proc. SPIE, Adv. Algorithms and Architectures for Signal Process. III*, Feb. 1988, pp. 368–376.

[3] H. B. Lee and M. S. Wengrovitz, "Improved high-resolution direction-finding through use of homogeneous constraints," in *Fourth Annual ASSP Workshop on Spec. Est. and Modeling*, Aug. 1988, pp. 152–157.

[4] H. B. Lee and M. S. Wengrovitz, "Resolution threshold of beamspace MUSIC for two closely spaced emitters," *IEEE Trans. Acoust., Speech, Signal Process.*, vol. 38, no. 9, pp. 1545–1559, Sept. 1990.

[5] X. L. Xu and K. M. Buckley, "Statistical performance comparison of MUSIC in element-space and beam-space," in *Proc. IEEE Intl. Conf. Acoust., Speech, and Signal Process.*, 1989, pp. 2124–2127.

[6] H. L. Van Trees, *Optimum array processing*, John Wiley & Sons, Inc., New York, 2002.

[7] M. D. Zoltowski, G. M. Kautz, and S. D. Silverstein, "Beamspace root-MUSIC," *IEEE Trans. Signal Process.*, vol. 41, no. 1, pp. 344–364, Jan. 1993.

[8] G. Xu, S. D. Silverstein, R. H. Roy, and T. Kailath, "Beamspace ESPRIT," *IEEE Trans. Signal Process.*, vol. 42, no. 2, pp. 349–356, Feb. 1994.

[9] Z. Guo, X. Wang, and W. Heng, "Millimeter-wave channel estimation based on 2-D beamspace MUSIC method," *IEEE Trans. Wireless Commun.*, vol. 16, no. 8, pp. 5384–5394, Aug. 2017.

[10] H. Zhao, N. Zhang, and Y. Shen, "Robust beamspace design for direct localization," in *IEEE Intl. Conf. Acoust., Speech and Signal Process.*, May 2019, pp. 4360–4364.

[11] P. P. Vaidyanathan and P.-C. Chen, "Convolutional beamspace for array signal processing," in *IEEE Intl. Conf. Acoust., Speech, and Signal Process.*, 2020.

[12] P.-C. Chen and P. P. Vaidyanathan, "Convolutional beamspace for linear arrays," *IEEE Trans. Signal Process.*, vol. 68, pp. 5395–5410, 2020.

[13] Po-Chih Chen and P. P. Vaidyanathan, "Convolutional beamspace and sparse signal recovery for linear arrays," in *Asilomar Conf. on Signal, Syst., Comput.*, 2020, pp. 929–933.

[14] P.-C. Chen and P. P. Vaidyanathan, "Sliding-Capon based convolutional beamspace for linear arrays," in *IEEE Intl. Conf. Acoust., Speech, and Signal Process.*, 2021.

[15] A. L. Swindlehurst, E. Ayanoglu, P. Heydari, and F. Capolino, "Millimeter-wave massive MIMO: the next wireless revolution?," *IEEE Commun. Mag.*, vol. 52, no. 9, pp. 56–62, Sept. 2014.

[16] X. Gao, L. Dai, and A. M. Sayeed, "Low RF-complexity technologies to enable millimeter-wave MIMO with large antenna array for 5G wireless communications," *IEEE Commun. Mag.*, vol. 56, no. 4, pp. 211–217, Apr. 2018.

[17] A. V. Oppenheim and R. W. Schafer, *Discrete-time signal processing*, Prentice Hall, 2010.

[18] P. P. Vaidyanathan, *Multirate systems and filter banks*, Prentice Hall, Englewood Cliffs, N.J., 1993.

[19] V. Pan, "Sequential and parallel complexity of approximate evaluation of polynomial zeros," *Computers & Mathematics with Applications*, vol. 14, no. 8, pp. 591–622, 1987.

[20] P. P. Vaidyanathan, S. Mitra, and Y. Neuvo, "A new approach to the realization of low-sensitivity IIR digital filters," *IEEE Trans. Acoust., Speech, Signal Process.*, vol. 34, no. 2, pp. 350–361, 1986.

[21] P. P. Vaidyanathan, P. Regalia, and S. Mitra, "Design of doubly-complementary IIR digital filters using a single complex allpass filter, with multirate applications," *IEEE Trans. Circuits Syst.*, vol. 34, no. 4, pp. 378–389, 1987.

[22] M. Renfors and T. Saramaki, "Recursive Nth-band digital filters–Part I: Design and properties," *IEEE Trans. Circuits Syst.*, vol. 34, no. 1, pp. 24–39, 1987.

[23] T. Q. Nguyen, T. I. Laakso, and T. E. Tuncer, "On perfect-reconstruction allpass-based cosine-modulated IIR filter banks," in *Proc. of IEEE Int. Symp. on Circuits and Syst.*, 1994, vol. 2, pp. 33–36.

[24] Xi Zhang, Wei Wang, T. Yoshikawa, and Y. Takei, "Design of IIR orthogonal wavelet filter banks using lifting scheme," *IEEE Trans. Signal Process.*, vol. 54, no. 7, pp. 2616–2624, 2006.

[25] Heinrich W. Lollmann and Peter Vary, "Design of critically subsampled DFT filter-banks with allpass polyphase filters and near-perfect reconstruction," in *IEEE Intl. Conf. Acoust., Speech and Signal Process.*, 2009, pp. 3185–3188.

[26] P. P. Vaidyanathan and T. Q. Nguyen, "Eigenfilters: a new approach to least-squares FIR filter design and applications including Nyquist filters," *IEEE Trans. Circuits Syst.*, vol. 34, no. 1, pp. 11–23, Jan. 1987.

[27] P. Stoica and A. Nehorai, "MUSIC, maximum likelihood, and Cramer-Rao bound," *IEEE Trans. Acoust., Speech, Signal Process.*, vol. 37, no. 5, pp. 720–741, May 1989.